

# Deformation and tribology of multi-walled hollow nanoparticles

U. S. Schwarz, S. Komura and S. A. Safran  
Department of Materials and Interfaces,  
Weizmann Institute of Science,  
Rehovot 76100, Israel

October 27, 2018

## Abstract

Multi-walled hollow nanoparticles made from tungsten disulphide ( $\text{WS}_2$ ) show exceptional tribological performance as additives to liquid lubricants due to effective transfer of low shear strength material onto the sliding surfaces. Using a scaling approach based on continuum elasticity theory for shells and pairwise summation of van der Waals interactions, we show that van der Waals interactions cause strong adhesion to the substrate which favors release of delaminated layers onto the surfaces. For large and thin nanoparticles, van der Waals adhesion can cause considerable deformation and subsequent delamination. For the thick  $\text{WS}_2$  nanoparticles, deformation due to van der Waals interactions remains small and the main mechanism for delamination is pressure which in fact leads to collapse beyond a critical value. We also discuss the effect of shear flow on deformation and rolling on the substrate.

## 1 Introduction

Graphite and layered material made from metal disulphides ( $\text{MoS}_2$ ,  $\text{WS}_2$ ) and similar composites ( $\text{MoSe}_2$ ,  $\text{WSe}_2$ , BN, etc.) are good lubricants since under shear the layers can easily slide over each other due to atomic smoothness and weak van der Waals (vdW) interactions [1]. Therefore they are widely used as solid lubricants or additives to liquid lubricants. However, finite sized crystallites in powders have edges with dangling bonds which can react chemically with the sliding surfaces. This problem can be avoided by

using hollow nanoparticles made from the same material, where the layers are not planar, but are bent into closed shells. It has been shown recently that multi-walled  $\text{WS}_2$  nanoparticles perform very well as additives [2, 3]. Closer investigations using the Surface Force Apparatus (SFA) revealed that  $\text{WS}_2$  layers are transferred onto the sliding surfaces by delamination of the nanoparticles [4]. These peeled layers form islands on which the Friction Force Microscope measured much smaller friction than on the surrounding mica. Hence multi-walled nanoparticles can act as reservoirs which release layers of low shear strength exactly where needed while avoiding too many dangling bonds.

A theoretical understanding of the mechanical properties of multi-walled hollow nanoparticles is important for future tribological applications. In this paper, we use scaling arguments based on continuum elasticity theory and pairwise summation of vdW interactions in order to investigate theoretically the effect of adhesion, pressure and shear flow on the deformation and mechanical stability of hollow nanoparticles of spherical shape. Figure 1 schematically depicts some of the aspects discussed in the following. We show that vdW adhesion to the substrate (as well as to each other) can be several orders of magnitude larger than thermal energies and scales linearly with radius, but is almost independent of thickness. Despite the large energy of adhesion, we find that for typical  $\text{WS}_2$  nanoparticles, coherent and even incoherent deformations due to the vdW adhesion to the substrate are only in the Angstrom range and will leave the nanoparticles basically intact. Thus for  $\text{WS}_2$  nanoparticles the vdW adhesion favors the release of delaminated layers onto the surfaces, but does not trigger the delamination itself. The main mechanism for delamination of  $\text{WS}_2$  nanoparticles is shown to be pressure which leads to a mechanical instability in linear elasticity theory. This might explain why damage of  $\text{WS}_2$  nanoparticles was found to occur only beyond a critical load [3]. We also show that shear flow does not lead to considerable deformation of  $\text{WS}_2$  nanoparticles and that very large shear rates are needed in order to make adhering particles roll in shear flow.

Similar methods have been used before to predict the shape of fullerenes [5, 6] and to account for the faceted shape of metal disulphide particles [7, 8]. Compared with *ab initio* methods [9], tight-binding schemes [10] and molecular simulations [11] which have been used before to investigate the mechanical properties of fullerene-like material, our approach has the advantage that it is asymptotically correct for large systems and universal in the sense that different material systems enter on the level of their elastic and vdW constants. In particular we discuss C,  $\text{MoS}_2$  and  $\text{WS}_2$ , although we focus on the  $\text{WS}_2$  nanoparticles used in the tribological experiments mentioned above. Our scaling approach allows us to predict how tribological performance depends

on radius  $R$ , shell thickness  $h$  and layer thickness  $a$  of the nanoparticles. We show that scaling with  $h$  does not result from the vdW contributions, but rather from the scaling of the elastic constants with  $h$ . Several critical quantities derived scale strongly with  $R/h$  for coherent deformation and with  $R/a$  for incoherent deformation. Hence tribological performance can be tuned by varying the concentration of defects (which switches between the coherent and incoherent regime) and the ratios  $R/h$  and  $R/a$ , respectively.

## 2 Preliminaries

In the following we consider hollow nanoparticles with outer radius  $R$  and thickness  $h$  which results from nesting several elastic shells of thickness  $a$  each. Typical  $\text{WS}_2$  particles used in tribological experiments have  $R \approx 60$  nm and  $h \approx 9.3$  nm (15 layers with an interlayer distance of  $a = 0.62$  nm,  $R/h \approx 6$ ,  $R/a \approx 100$ ). In fig. 2 a high resolution transmission electron micrograph of a  $\text{WS}_2$  nanoparticle with 11 layers is shown. The elastic shells are closed since their formation is driven by the energy reduction due to the absence of dangling bonds. In order to achieve closure, topology dictates that for carbon shells 12 pentagons have to be inserted into the graphite network of hexagons. For hexagonally layered composites, the sheets have a more complicated molecular structure (typically triple layers) and different kinds of defects have to occur to ensure closure. In our continuum approach, we assume that defects are distributed in a homogeneous way to give a spherical shape with a certain preferred radius  $R$  [7]. Similar approaches to fullerene-like particles have considered sheets which are planar in equilibrium; in order to account for their curvature, they explicitly considered defects [5, 6, 7, 8]. However, in this approach the elastic response of a spherical shell is very complicated and no unifying scaling approach is possible.

The new feature of the elasticity of a closed shell with a preferred radius  $R$  is that stretching is a first-order effect and the spherical shell cannot be bent without being stretched [12]. This interplay between bending and stretching has been studied before for thermal fluctuations of polymerized vesicles [13]. The elastic behavior of the shell is determined by two contributions: bending energy  $E_b \sim \kappa \int dA c^2$  with bending rigidity  $\kappa$  and mean curvature  $c$ , and stretching energy  $E_s \sim G \int dA e^2$  with in-plane stretching modulus (or two-dimensional Young modulus)  $G$  and in-plane strain  $e$ . Here  $\int dA$  represents the surface integral; the elastic contributions in shell theory follow by integrating over the thickness of the shell. Consider a spherical shell of radius  $R$  which is expanded by  $\Delta R$ . Then  $c$  changes by  $\Delta R/R^2$  and  $e$  by  $\Delta R/R$ , thus both contributions are first order effects. Since  $E_b/E_s \sim \kappa/GR^2$ , the rela-

tive strength of bending and stretching depends both on material parameters and radius; on large length scales  $R \gg (\kappa/G)^{1/2}$  and stretching will always dominate.

In the framework of continuum elasticity theory, the elastic moduli  $\kappa$  and  $G$  can be calculated from the in-plane stretching elastic constant  $C_{11}$  of the corresponding hexagonal layered material as  $\kappa = C_{11}h^3/12$  and  $G = C_{11}h$  [7]. The values for  $C_{11}$  are 1060, 238 and  $150 \times 10^{10}$  erg/cm<sup>3</sup> for C, MoS<sub>2</sub> and WS<sub>2</sub>, respectively [14]. The same scaling with  $h$  is found for thin films made from isotropic elastic material [12]. It only applies for coherent bending of the different layers; for incoherent bending, slip occurs between adjacent layers and overall bending becomes easier. The bending rigidity then follows as  $\kappa \sim C_{11}a^3(h/a) = C_{11}a^2h$  where  $a$  is the effective thickness of a single layer [7]. It should be of the same order of magnitude, but somewhat smaller than the interlayer distance (which is 3.4 Å for C and 6.2 Å for MoS<sub>2</sub> and WS<sub>2</sub>). Note that the in-plane modulus  $G \sim C_{11}a(h/a) = C_{11}h$  stays the same since it scales linearly with thickness. The change from coherent to incoherent bending can be considered to be defect mediated; dislocations will proliferate for increasing thickness and finally will lead to grain boundaries which account for the typical faceted shape seen in fig. 2 [7].

### 3 Adhesion

We consider a substrate which interacts by attractive vdW forces with a film of thickness  $h$  which is a distance  $D$  away from the substrate. Pairwise integration of the potential  $-A/\pi^2r^6$  (where the Hamaker constant  $A$  is typically of the order of  $10^{-12}$  erg) over the two volumes yields the vdW energy per unit area

$$u = \frac{A}{12\pi} \frac{h(h+2D)}{D^2(h+D)^2}. \quad (1)$$

Here  $D$  is an atomic cutoff for the vdW interaction which in the following is chosen to be 1.65 Å [15]. Although the adhesion energy  $u$  scales linearly with  $h$  for small  $h$ , for more than one layer we have  $h > D$  and  $u$  saturates at a constant value  $u = A/12\pi D^2 \approx 100$  erg/cm<sup>2</sup>. For the case of a single layer, one can replace the volume integral over the film by a surface integral times the effective thickness  $h$ ; this is equivalent to considering  $h \ll D$  in eq. (1) and leads to  $u = Ah/6\pi D^3$ . Since  $D$  and  $h$  are of the same order of magnitude, we essentially recover the result for a multi-layered film. Hence we conclude that due to the rapid saturation of the vdW binding energy with increasing  $h$ , for multi-layered films under adhesion conditions no considerable scaling with  $h$  is expected from the vdW terms.

It can be shown by similar arguments (*e.g.* by using eq. (1) within the Derjaguin approximation) that the energy of a hollow nanoparticle adhering to a substrate does not depend on  $h$  as long as  $h \gtrsim D$ . Then the adhesion energy equals the vdW energy of close approach between a sphere and a substrate,  $E_A = AR/6D$  [15]. Using values for  $A$ ,  $D$  and  $R$  as given above yields  $E_A = 6 \times 10^{-11}$  erg = 1400 kT. The energy of adhesion between two particles is only a factor of 2 smaller than the one between a particle and the substrate, and hence well above thermal energies as well. We thus conclude that the vdW interaction leads to considerable adhesion of the particles to the substrate and to each other. The same holds true for peeled off outer layers: with  $R = 60$  nm, the energy of adhesion can be estimated to be  $R^2u = 10^5$  kT.

## 4 Deformation under adhesion

The onset of delamination can be estimated by considering large deformations of the nanoparticles. We do not offer a theory for fracture and estimate the limit of mechanical stability by an internal criterion within our continuum description: fracture and delamination sets in when so much stress has accumulated that the deformation becomes of the order of the radius. Determining the deformation of a spherical elastic shell is a difficult problem which depends on prestress, elastic constants and size as well as on the nature of the deforming force. Here we discuss the deformation on a substrate for two cases which can be treated in the framework of our scaling approach. In the following  $H$  is the indentation. For small deformations  $H < h$  (fig. 3a), the shell flattens at the bottom. For large deformations  $H > h$  (fig. 3b), a contact disc with radius  $r$  develops and the elastic energy is localized in the circular fold surrounding it. The respective elastic energies are [12]

$$E_{small} \sim \frac{G^{1/2}\kappa^{1/2}}{R}H^2, \quad E_{large} \sim \frac{G^{1/4}\kappa^{3/4}}{R}H^{3/2}. \quad (2)$$

Here we neglect a bending term  $\sim \kappa H/R$ . We also assumed that due to low friction, slip can occur between the contact disc and the substrate; otherwise compression energy  $\sim GH^3/R$  would accumulate in the contact disc. The rest of the relaxing shell is assumed to keep a spherical form with radius  $R' > R$  in order to keep area constant and to avoid compression energy. However, the difference is  $(R' - R) \sim H^2/R$  and can be shown to be negligible in the following.

If the deformations are driven by vdW adhesion, the energy gained on adhesion can be shown to scale as  $E_A \sim uRH$  for both small and large

deformations. Setting this adhesion energy equal to the estimates for the elastic energies from eq. (2) yields estimates for indentation:

$$H_{small} \sim \frac{R^2 u}{G^{1/2} \kappa^{1/2}} \sim \left( \frac{u}{C_{11} h} \right) \left( \frac{R}{h} \right) R, \quad H_{large} \sim \frac{R^4 u^2}{G^{1/2} \kappa^{3/2}} \sim \left( \frac{u}{C_{11} h} \right)^2 \left( \frac{R}{h} \right)^3 R. \quad (3)$$

Here and in the following we will always give the result both in terms of the elastic moduli and their scaling with thickness for coherent bending. The dimensionless quantity  $u/C_{11}h$  is the ratio of van der Waals adhesion energy to two-dimensional Young modulus and will be of order  $10^{-4}$  for the WS<sub>2</sub> nanoparticles. In this case we are in the regime  $H < h$  and deformations will be in the Angstrom range. Thus delamination cannot be expected to be caused by adhesion. For incoherent bending,  $R/h$  has to be replaced by  $R/a$  in both regimes.

One system for which vdW adhesion leads to strong deformations are *single-walled* hollow nanoparticles. In this case, care has to be taken to use the correct values for  $G$  and  $\kappa$ . Since  $G$  is a purely two-dimensional quantity,  $G = C_{11}h$  can be used where  $h$  is identified with the interlayer distance. However,  $\kappa$  has to be extracted from molecular calculations [5, 10, 11]. For carbon, one finds  $G = 3.6 \times 10^5$  erg/cm<sup>2</sup> and  $\kappa \approx 1.6 \times 10^{-12}$  erg  $\approx$  40 kT. For both MoS<sub>2</sub> and WS<sub>2</sub>,  $G$  is smaller by a factor 4 and  $\kappa$  is larger by a factor 10. In all three cases, for radii larger than a few nm considerable deformations arise. The critical radius  $R_c$  where indentation  $H$  and radius  $R$  become of the same magnitude follows from the second relation of eq. (3) as  $R_c \sim G^{1/6} \kappa^{1/2} u^{-2/3}$ . For C, we find  $R_c \approx 5$  nm and for the metal disulphides  $R_c \approx 10$  nm. For nanotubes, we find similar results which are in good agreement with experiments and molecular calculations [16, 17].

## 5 Deformation under pressure

We now proceed to show that pressure can lead to an instability which could account for the observed delamination. We consider the formation of a contact disc for a shell which is pressed onto the substrate by pressure in the surrounding liquid. The corresponding energy is  $E_p \sim -pRH^2$ , thus it scales more strongly with  $H$  than the restoring elastic energy  $E_{large}$  in eq. (2). This scaling indicates an instability: small deformations are suppressed, but large deformations grow without limits beyond the critical indentation  $H_c$  where  $E_{large} + E_p$  attains a maximum [12]. Setting  $H_c = R$  gives an estimate for

the critical pressure for delamination:

$$p_c \sim \frac{G^{1/4} \kappa^{3/4}}{R^{5/2}} \sim C_{11} \frac{h}{R} \left( \frac{h}{R} \right)^{3/2}. \quad (4)$$

Using typical values gives  $p_c \approx 1.7$  GPa. Incoherent deformations can be treated by replacing  $(h/R)^{3/2}$  by  $(a/R)^{3/2}$  in eq. (4) and hence would decrease the estimate to 25 MPa. Although a full treatment of the instability requires a theory for the non-linear elasticity, we can still suggest that pressure will be a very likely mechanism to cause delamination. This prediction agrees nicely with the experimental observation that damage sets in at a finite threshold of the load [3]. Note that for single-walled buckyballs  $C_{60}$  with  $R = 3.55 \text{ \AA}$ , eq. (4) gives  $p_c = 15$  GPa which is in surprisingly good agreement with the value 20 GPa found experimentally [18].

Although the pressure values estimated here seem to be high, they refer to particles of nm-size, and the corresponding forces are of the order of  $10^{-3}$  dyn. In friction experiments, the pressures and forces needed for delamination are most likely to occur near asperities. This might explain why delamination has been observed in the SFA only when shearing the two surfaces [4]: the nanoparticles then behaves as granular material which gets jammed and pressure and forces become localized.

## 6 Shear flow

Since the  $WS_2$  nanoparticles are immersed in liquid lubricant in strong motion, we finally consider the effect of shear flow. Balancing the deforming viscous force with the elastic restoring force and setting the resulting deformation equal to the radius gives an estimate for the shear rate at which delamination sets in. For  $h < R$ , we find that only stretching is relevant and that the critical shear rate is

$$\dot{\gamma}_c \sim \frac{G}{\eta R} \sim \frac{C_{11}}{\eta} \frac{h}{R}. \quad (5)$$

Using viscosity  $\eta \approx 1$  cP (which applies both to water and mineral oil), we find  $\dot{\gamma}_c \sim 2.5 \times 10^{13}$  Hz. Such high shear rates are unattainable even near contacting asperities in macroscopic friction experiments, thus delamination is not likely to occur due to shear flow alone.

Shear flow past nanoparticle adhering to a substrate can cause them to roll. The particle begins to roll if the viscous drag evaluated at the midpoint,  $F_S = 6\pi\eta R^2 \dot{\gamma}$ , equals the friction force  $F_F$  caused by the adhesive load

$F_A = 2\pi Ru$ . Assuming Amontons' law for rolling friction,  $F_F = \mu F_A$ , we find

$$\dot{\gamma}_c = \frac{\mu u}{3\eta R} \quad (6)$$

where the coefficient of rolling friction  $\mu$  can be taken to have the typical value  $10^{-3}$ ; then  $\dot{\gamma}_c$  is of the order of  $5 \times 10^5$  Hz. This value is higher than typical shear rates probed with the SFA ( $v = 10 \mu\text{m/s}$ ,  $\dot{\gamma} = 10^4$  Hz on nm-separation), but certainly lower than shear rates occurring near the asperities of macroscopic friction experiments ( $v = 1\text{m/s}$ ,  $\dot{\gamma} = 10^9$  Hz on nm-separation).

## 7 Conclusion

We have shown that in friction experiments with multi-walled hollow nanoparticles, delamination is likely to be caused by pressure. When nanoparticles delaminate, dangling bonds develop as they do for powders from layered material. However, there are two reasons why they should be less problematic. First delamination takes place with one or two layers and the density of dangling bonds remains low. Second we showed that delamination may occur under adhering conditions. The adhesion (and possibly the shear) will cause the layers to align parallel to the substrate, in contrast to the powders where the orientation is preferentially perpendicular to the substrate. It has been shown experimentally that delaminated layers from nanoparticles form islands while platelets form a thicker, more disorganized film [4]. Our scaling approach shows that there are two control parameters which might be used for tribological optimization: the ratio of radius to thickness and the concentration of defects (that determine the regimes of coherent and incoherent bending).

Using nanoparticles as additives to liquid lubricants raises interesting questions about the role of wetting. The lubricant used in the friction experiments mentioned is a bad solvent for the nanoparticles, which provides an additional force to drive them onto the substrate. A dewetted region is expected to form between the adhering particle and the substrate; like a capillary bridge in a good wetting situation, it might enhance adhesion.

## Acknowledgments

We thank C. DRUMMOND, Y. GOLAN, J. ISRAELACHVILI, J. KLEIN, G. SEIFERT and especially R. TENNE for helpful discussions. R. TENNE kindly provided the electron micrograph shown in fig. 2. SAS thanks the Gerhard



M.J. Schmidt Minerva Center for Supramolecular Architecture for support. SK thanks the Ministry of Education, Science and Culture, Japan for providing financial support during his visit to Israel. USS gratefully acknowledges support by the Minerva Foundation.

## References

- [1] Singer I. L. and Pollock H. M., *Fundamentals of Friction: Macroscopic and Microscopic Processes* (Kluwer, Dordrecht) (1992).
- [2] Rapoport L., Bilik Y., Feldman Y., Homyonfer M., Cohen S. R. and Tenne R., *Nature* **387** 791 (1997).
- [3] Rapoport L., Feldman Y., Homyonfer M., Cohen H., Sloan J., Hutchison J. L. and Tenne T., *Wear* **225-229** 975 (1999).
- [4] Golan Y., Drummond C., Homyonfer M., Feldman Y., Tenne R. and Israelachvili J., *Adv. Mat.* **11** 934 (1999); Drummond C., Alcantar N., Israelachvili J., Tenne R. and Golan Y., Preprint (1999).
- [5] Tersoff J., *Phys. Rev. B* **92** 15546 (1992).
- [6] Witten T. A. and Li H., *Europhys. Lett.* **23** 51 (1993).
- [7] Srolovitz D. J., Safran S. A. and Tenne R., *Phys. Rev. E* **49** 5260 (1994).
- [8] Srolovitz D. J., Safran S. A., Homyonfer M. and Tenne R., *Phys. Rev. Lett.* **74** 1779 (1995).
- [9] Adams G. B., Sankey O. F., Page J. B., O’Keeffe M. and Drabold D. A., *Science* **256** 1792 (1992).
- [10] Hernandez E., Goze C., Bernier P. and Rubio A., *Phys. Rev. Lett.* **80** 4502 (1998); Seifert G., Terrones H., Terrones M., Jungnickel G. and Frauenheim T., Preprint (1999).
- [11] Yakobson B. I., Brabec C. J. and Bernholc J., *Phys. Rev. Lett.* **76** 2511 (1996).
- [12] Landau L. D. and Lifshitz E. M., *Theory of Elasticity* (Pergamon Press, Oxford) (1970).
- [13] Komura S. and Lipowsky R., *J. Phys. II France* **2** 1563 (1992); Zhang Z., Davis H. T. and Kroll D. M., *Phys. Rev. E* **48** R651 (1993).

- [14] Landolt and Börnstein, *Units and Fundamental Constants in Physics and Chemistry* (Springer, Berlin) (1991).
- [15] Israelachvili J. N., *Intermolecular and Surface Forces* (Academic Press, London) (1992).
- [16] Ruoff R. S., Tersoff J., Lorents D. C., Subramoney S. and Chan B., *Nature* **364** 514 (1993).
- [17] Our calculation for nanotubes is not given here since deformations of cylindrical shells are conceptually different from the ones of spherical shells: for spherical shells, the balance of stretching and bending leads to localization of deformation. For cylindrical shells, stretching can be avoided and non-local bending has to be considered.
- [18] Nunez-Regueiro M., *Mod. Phys. Lett. B* **6** 1153 (1992).

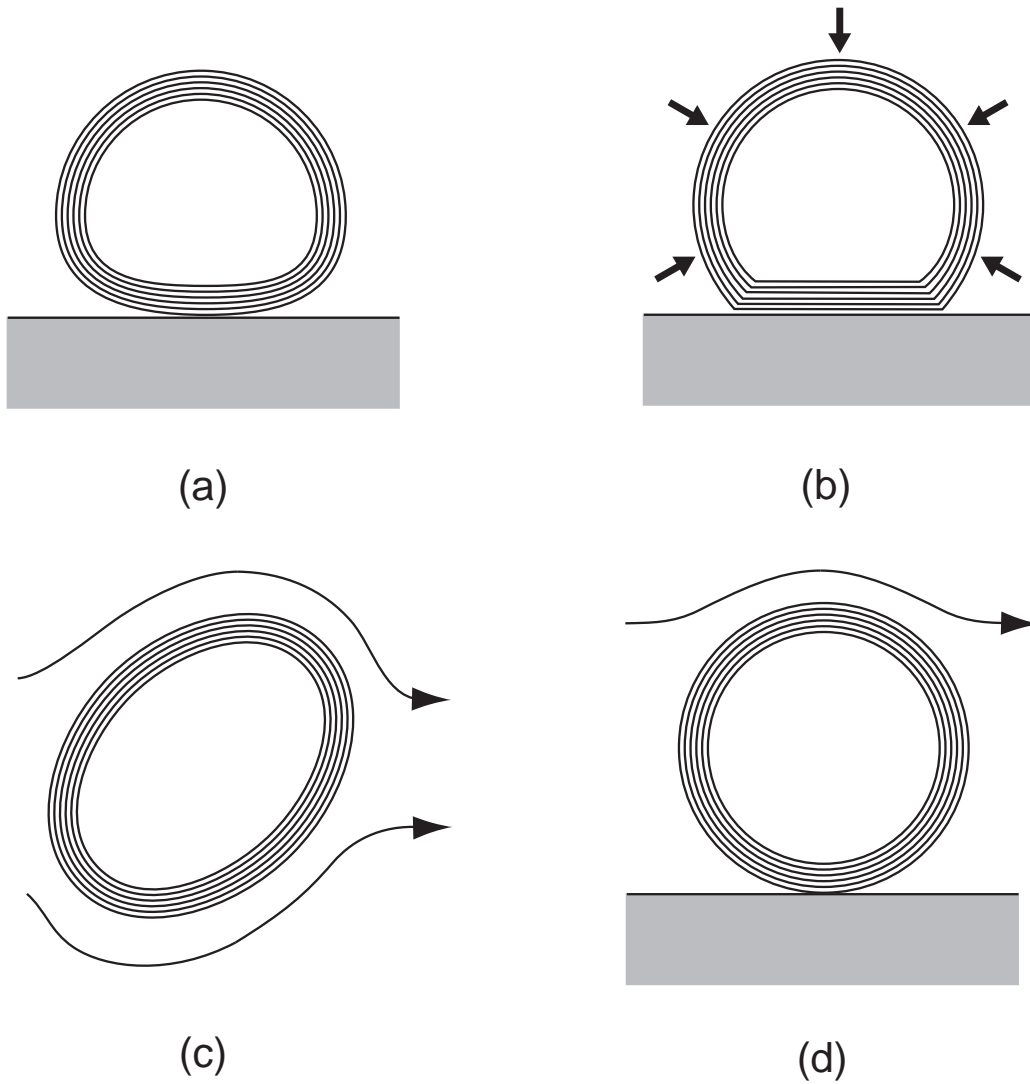


Figure 1: Several aspects of friction experiments with multi-walled nanoparticles: (a) weak deformation due to adhesion onto a substrate, (b) strong deformation due to pressure, (c) deformation in shear flow and (d) rolling of adhering particles in shear flow.

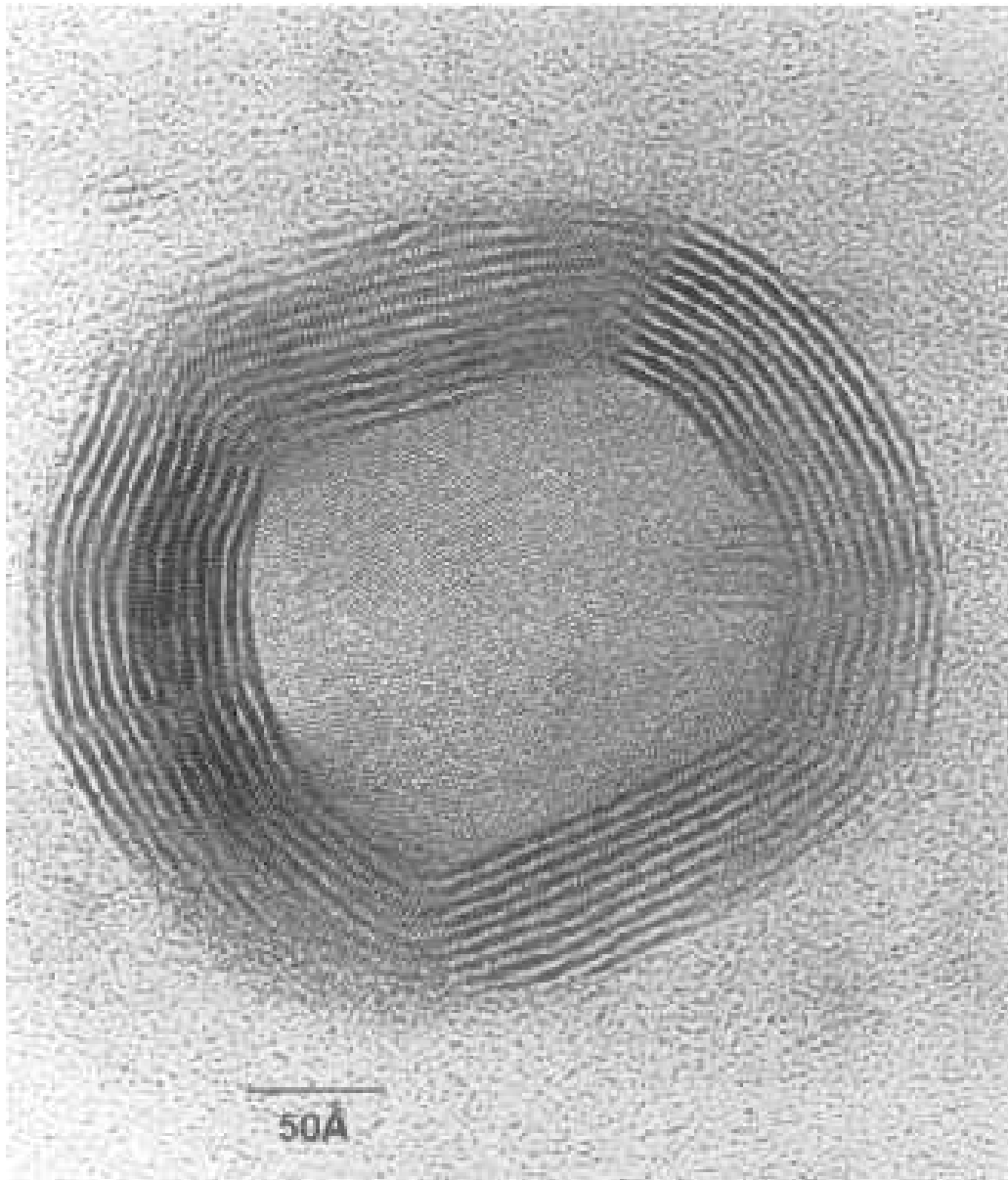


Figure 2: High resolution transmission electron micrograph of a multi-walled WS<sub>2</sub> nanoparticle. The slightly faceted shape is typical and can be attributed to the assembly of defects into grain boundaries [7].

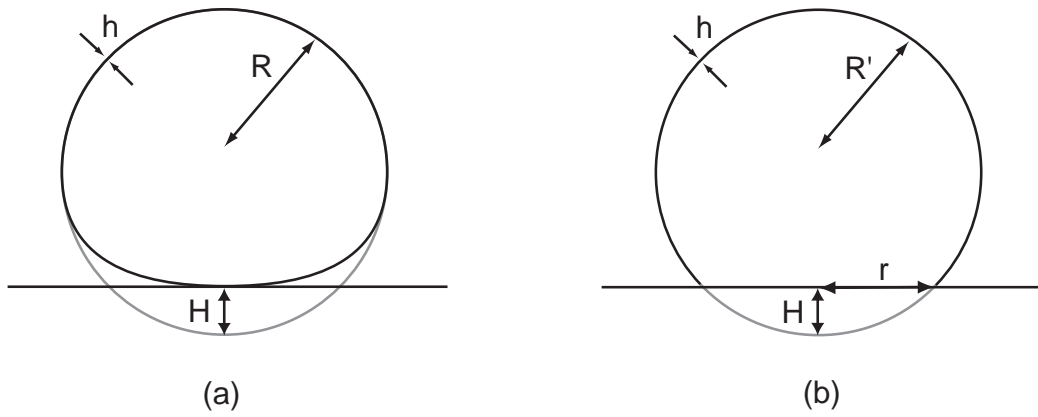


Figure 3: Possible deformations of a spherical elastic shell on contact with a substrate: (a) flattening and (b) contact disc.  $R$  is the initial particle radius,  $R'$  the radius after flattening,  $h$  the shell thickness,  $H$  the indentation and  $r$  the radius of the contact disc. For small  $H$ , one finds geometrically  $r^2 = 2HR'$ .